Heat transport through diffusive interfaces

Jason D. Flanagan,[1] Angela S. Lefler,[1] and Timour Radko[1]

Received 22 February 2013; revised 27 March 2013; accepted 31 March 2013; published 31 May 2013.

[1] We perform a series of 3-D Direct Numerical Simulations (DNS) to assess the vertical heat transport through thermohaline staircases in the Arctic Ocean. The diagnostics of DNS, performed for the first time in the realistic parameter range, result in vertical fluxes exceeding those of extant "four-thirds flux laws" by as much as a factor of 2 and suggest that the 4/3 exponent may require downward revision. Through a series of equivalent 2-D DNS, we show that they are consistent with their more resource-intensive 3-D counterparts for sufficiently large density ratio (R_ρ) but underestimate heat transport for low R_ρ. Finally, we examine the role of boundary conditions in controlling the vertical heat transport. Rigid boundaries—a necessary ingredient in laboratory-derived flux-laws—are shown to reduce the estimates of heat fluxes relative to the corresponding periodic boundary conditions. **Citation:** Flanagan, J. D., A. S. Lefler, and T. Radko (2013), Heat transport through diffusive interfaces, *Geophys. Res. Lett.*, *40*, 2466–2470, doi:10.1002/grl.50440.

1. Introduction

[2] The Arctic Ocean has been the subject of increasing interest in recent years due to the observed reduction of sea-ice thickness and spatial coverage. *Turner* [2010] has shown that there is enough heat within an observed intruding layer of warm Atlantic Water (AW) to melt all Arctic sea-ice within 4 years if this heat could be brought to the surface at once. The mechanisms controlling the rate of heat transfer are poorly understood, and here, we examine one of the mixing agents - diffusive convection. The stratified cold halocline overlying the AW is prone to double-diffusion, the small-scale mixing phenomenon driven by the difference in molecular diffusivities of heat and salt. It is the diffusive convection mode of double-diffusion, where fluid is hydrostatically stable despite an unstable thermal gradient that is prevalent in the central Arctic (Canada Basin). Double-diffusion is ultimately responsible for the appearance of well-defined thermohaline staircases that are known to elevate the vertical heat transport relative to smooth-gradient stratifications. Recent Ice-Tethered Profiler (ITP) data have revealed staircases that are prevalent throughout the Canada Basin—~95% of ITPs show staircases at the depth range 200–300 m [*Timmermans et al*., 2008].

[3] Numerous theoretical studies and laboratory experiments have focused on the dynamics and consequences of diffusive convection in the Arctic region [e.g., *Timmermans et al*., 2008; *Caro*, 2009; *Turner*, 2010; *Kwok and Untersteiner*, 2011]. *Turner* [2010] concludes that diffusive convection has contributed significantly to the observed increase in sea-ice melting during the past few decades, while *Kwok and Untersteiner* [2011] have noted that the surplus heat needed to explain the loss of Arctic sea-ice, over this period, is on the order of 1 W/m^2.

[4] Earlier laboratory experiments [e.g., *Turner*, 1973; *Marmorino and Caldwell*, 1976; *Linden and Shirtcliffe*, 1978; *Kelley*, 1990] have produced estimates of vertical heat transport based on the so-called "4/3 flux laws" of the form

$$\alpha F_T = C(R_\rho)\left(g\kappa_T^2/\nu\right)^{1/3}(\alpha\Delta T)^{4/3} \quad (1)$$

where it is assumed that vertical heat transport is controlled by the temperature and salinity differences between two adjacent layers, and the layer thickness plays a secondary role. Here, κ_T is the molecular diffusivity of heat, ν is kinematic viscosity, g is gravity, α is the coefficient of thermal expansion and the flux law coefficient C is fully determined by the density ratio $R_\rho = \beta\Delta S/\alpha\Delta T$. Recent temperature and salinity measurements of the Arctic Ocean double-diffusive staircase gathered by a number of Ice-Tethered Profilers (ITP) provide a thorough spatial coverage of the Beaufort Gyre and facilitate application of laboratory-based predictions [*Krishfield et al*., 2006]. For instance, the laboratory-calibrated 4/3 flux law [*Kelley*, 1990] has been used, in conjunction with ITP data by *Timmermans et al*. [2008] who arrived at heat flux (F_H) estimates through each step in the range 0.05–0.3 W/m^2 with the average value of 0.22 W/m^2. Even such low values of heat flux are likely to affect the dynamics and heat budget of the Arctic Ocean [*Turner*, 2010]. However, the accuracy of laboratory-based estimates in application to oceanic staircases has been questioned for several reasons—the difference in scales, presence of rigid boundaries, and run-down setup of experiments—motivating our attempt at alternative estimates of the vertical heat transport.

[5] 3-D direct numerical simulations (DNS) are proving to be the new standard for analysis of thermohaline staircases and the advective processes that transport heat upwards across diffusive interfaces. To provide reliable estimates of heat transport, simulations should meet a set of stringent requirements. In particular, simulations should (i) be performed at a resolution that adequately represents the scales of salt dissipation, (ii) utilize sufficiently large computational domains that replicate typical step-sizes in the Arctic staircase, and (iii) be performed over a time period long enough to provide accurate statistical description. Such requirements are so computationally expensive that, until now, DNS of Arctic staircases have been unfeasible. Modelers had to either resort to 2-D simulations or to compromise in their choice of parameters (use unrealistic values of diffusivity ratio or step heights, for instance). *Caro*

[1]Department of Oceanography, Naval Postgraduate School, Monterey, California, USA.

Corresponding author: J. D. Flanagan, Department of Oceanography, Graduate School of Engineering and Applied Sciences, Naval Postgraduate School, Monterey, CA 93943, USA. (jdflanag@nps.edu)

0094-8276/13/10.1002/grl.50440

[2009] performed DNS of a fluid with *periodic* boundary conditions and unrealistically high diffusivity ratio ($\tau = \kappa_S/\kappa_T$). He extrapolated high-tau simulations to evaluate the vertical heat transport for Arctic conditions and found it to be significantly larger than inferred from laboratory experiments. *Carpenter et al*. [2012] performed a series of 3-D DNS that differed from those of *Caro* [2009] in the model configuration through the inclusion of *rigid* boundaries. As a result, their DNS experienced a run-down evolution of the diffusive interface, a feature that is compatible with the laboratory configuration but which may not be realized in oceanic staircases. However, *Carpenter et al*. [2012] also showed that the laboratory-based flux laws predict lower heat transport than observed in their simulations and a stronger dependence on density ratio (R_ρ).

[6] Both the results of *Caro* [2009] and *Carpenter et al*. [2012] bring into question the relevance of lab-based flux laws when applied to Arctic staircases, a doubt that provides much motivation for this manuscript. Furthermore, if new estimates predict heat fluxes that are significantly higher than previously thought, then this could help explain the current heat surplus in the Arctic and illustrate the larger role diffusive convection plays in transporting warmer Atlantic water vertically to the surface sea-ice [*Turner*, 2010].

[7] To this end, we have taken 3-D DNS a significant step further by (i) utilizing a mesh-size that sufficiently resolves the scale of salt dissipation for realistic diffusivity ratio (i.e., $\tau = 0.005$), (ii) increasing the domain size to accurately reflect step-sizes in an actual staircase (H ~ 4 m), (iii) allowing our DNS to run for a time period that ensures accurate diagnostics, and (iv) ensuring that all parameters and conditions, such as a lack of rigid boundaries, are reflective of those found in the Arctic. Such a set-up has allowed us to derive flux laws that are more representative of real-world conditions. We have also tested the assumed 4/3 power dependence of extant flux laws through a series of DNS for various step heights in the range relevant to Arctic staircases and found that this exponent may require adjustment. Additionally, we have compared the results from 2-D DNS with those from the corresponding 3-D DNS and find that they are adequate for a range of relatively large R_ρ, but underestimate heat transport for relatively low ($R_\rho < 3$) density ratios. Finally, we have examined equivalent DNS with periodic and rigid boundary conditions and find that the choice of boundary conditions significantly affects fluxes.

[8] This manuscript is organized as follows: In section 2, we describe the models used for all DNS conducted. In section 3, we present the results; and in section 4, we summarize and discuss the main findings.

2. Model Description

[9] We first make use of a decomposition of the temperature and salinity fields into the linear basic state $(\bar{T}, \bar{S})$ and perturbation (*T,S*). The relevant equations are then the Boussinesq equations of motion [e.g., *Stern et al*., 2001] where, we note, the effects of compressibility and nonlinearities of the equation of state are not considered. The governing equations are expressed in terms of T and S and non-dimensionalized using the "standard" double-diffusive system: $l = (\kappa_T \nu / g\alpha \bar{T}_z)^{1/4}$ (length), l^2/κ_T (time), κ_T/l (velocity), and $\rho_0 \nu \kappa_T / l^2$ (pressure). Here, $\bar{T}_z$ is the temperature gradient and ρ_0 is the reference density used in the Boussinesq approximation. Finally, αT and βS are both scaled by $\alpha \bar{T}_z l$, leading to the set of equations

$$\frac{1}{Pr}\left(\frac{\partial \mathbf{u}}{\partial t} + \mathbf{u}\cdot\nabla\mathbf{u}\right) = -\nabla p + (T - S)\mathbf{k} + \nabla^2\mathbf{u}, \tag{2}$$

$$\nabla\cdot\mathbf{u} = 0, \tag{3}$$

$$\frac{\partial T}{\partial t} + \mathbf{u}\cdot\nabla T - \mathbf{k}\cdot\mathbf{u} = \nabla^2 T, \tag{4}$$

$$\frac{\partial S}{\partial t} + \mathbf{u}\cdot\nabla S - R_\rho \mathbf{k}\cdot\mathbf{u} = \tau\nabla^2 S \tag{5}$$

where $\mathbf{u}$ denotes the velocity field and $Pr = \nu/\kappa_T$, $\tau = \kappa_S/\kappa_T$, and $R_\rho = \beta\bar{S}_z/\alpha\bar{T}_z$ are the Prandtl number, molecular diffusivity ratio, and density ratio, respectively. These three non-dimensional numbers govern the evolution of the above system. System (2)–(5) has been solved using a parallelized pseudo-spectral code [*Stern and Radko*, 1998] with periodic boundary conditions for (*T,S*,$\mathbf{u}$). The background stratification $(\bar{T}_z, \bar{S}_z)$ is maintained throughout the experiment, thereby replicating conditions in the ocean where the influences of boundaries are minimal. For the purpose of evaluating the influence of boundary conditions, a different version of the model has been considered in which rigid stress-free boundaries are assumed in all spatial dimensions, with minimal changes to the underlying code.

[10] Throughout this study, we conduct one-layer DNS with parameter settings that reflect those found in the vicinity of the Beaufort Gyre in the Arctic Ocean. Recently, ITPs in the Arctic have recorded temperature and salinity profiles that clearly show stepped patterns at depths 200–300 m with typical layer thicknesses on the order of 1 - 10m [*Timmermans et al*., 2008] throughout the region. Parameter values typical to this area are $\bar{T}_z = 1.361 \times 10^{-2}\,^\circ\mathrm{Cm}^{-1}$, $\rho = 1.0289 \times 10^3$ kg m^{-3}, $C_p = 3844$ J kg^{-1} °C^{-1}, $\nu = 1.8$ 10^{-6}m^{2}s^{-1}, $\kappa_T = 1.4 \times 10^{-7}$m^{2}s^{-1}, $\kappa_S = 7 \times 10^{-10}$m^{2}s^{-1}, and $\alpha = 5.625 \times 10^{-5}$ °C^{-1}. Thus, $l = 1.35 \times 10^{-2}$m, $Pr = 13$, and $\tau = 0.005$. Such low values for l and τ present difficulties for any DNS that hopes to resolve scales down to the dissipation of salt ($l\sqrt{\tau}$). In what follows, the chosen grid scale (dz) is much less than that of temperature (l) and is comparable to that of salt.

3. Results

[11] To determine the vertical heat transport in the configuration that is consistent with typical staircases in the Beaufort Gyre of the Arctic Ocean, we have conducted 6 one-layer 3-D DNS each with a different R_ρ chosen from [2,3,4,6,8,10] for $Pr = 13$ and $\tau = 0.005$. Each experiment was initialized by a step-like *T-S* distribution at rest, perturbed by small-amplitude computer-generated random noise and conducted on the triply-periodic domain $\Omega = [0,300] \times [0,150] \times [0,300]$ (corresponding to the dimensional box ~4m × 2m × 4m) and a mesh of size $768 \times 384 \times 3072$. We have performed equivalent 2-D DNS for identical and increased aspect ratio, at both equal and twice the resolution, and found that heat fluxes remain largely unaffected, giving us confidence that our chosen domain size and resolution are adequate.

Figure 1. An example 3-D volume rendering of output from the MPI-based pseudo-spectral code used throughout this study. Shown is the instantaneous temperature perturbation field from a one-layer 3-D DNS with $\tau = 0.005$. Two identical layers are shown to illustrate the periodic nature of the system.

[12] Figure 1 presents the typical distribution of the total temperature $\bar{T} + T$ realized in 3-D DNS. This visualization reflects the interaction between regular, nearly flat interfaces and disorganized convective plumes advecting temperature and salinity through the well-mixed layers. For each DNS, temperature flux averaged over the whole computational domain ($F_{T\ \mathrm{nondim}} = -\overline{wT}$) was recorded and smoothed in time using the running average period of 20 non-dimensional units to remove high-frequency oscillations. In Figure 2a, we plot the corresponding dimensional heat flux ($F_{H\ \mathrm{dim}}$) as a function of dimensional time (t, in hours) for the DNS with $R_\rho = 4$. Non-dimensional units used by the model were converted to dimensional heat flux using $F_{H\ \mathrm{dim}} = \rho C_p \kappa_T\, dT/dz\, F_{T\ \mathrm{nondim}}$. After an initial period ($0 < t < 2.2$ hrs) of flux growth (corresponding to the emergence of the first diffusive plumes), the system quickly settles down to a state of near-equilibrium, with fluxes fluctuating about a mean value. Each of the six DNS illustrated the same behavior. In each case, the system was allowed to evolve far beyond the initial surge in flux so that an accurate time-mean value ($\overline{F_{H\ \mathrm{dim}}}$) could be ascertained. For consistency, we have considered the identical averaging range 4 hrs $< t <$ 18 hrs in all six cases. The finite time-record error estimated from the convergence pattern of our means is in the range 2–10% for all six DNS. An examination of our necessarily sparse saved data set indicates that the laminar transport through the interface is close to, but somewhat less than, the net flux (within a factor of two).

[13] In order to interpret our results in terms of the previous estimates of heat transport, we now compare the numerical fluxes with those inferred from laboratory experiments. Two commonly-used lab-derived heat flux-laws [*Marmorino and Caldwell*, 1976; *Kelley* 1990] are based on the 4/3 flux law (1) and assume the following flux law coefficients

$$C_{MC}(R_\rho) = 0.00859 \exp\{4.6 \exp[-0.54(R_\rho - 1)]\}, \quad (6)$$

and

$$C_K(R_\rho) = 0.0032 \exp\left\{4.8 R_\rho^{-0.72}\right\} \quad (7)$$

respectively. In Figure 2b, we compare heat fluxes diagnosed from our DNS with those from (6)–(7) for a range of density ratios. This comparison indicates that for low R_ρ, laboratory estimates enjoy some success in estimating F_H —for instance, at $R_\rho = 2$, *Kelley's* [1990] law is within

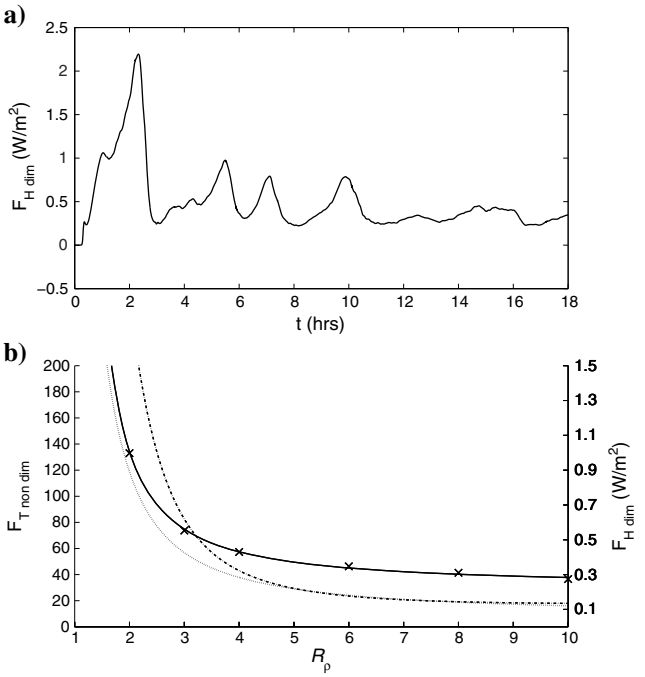

Figure 2. (a) Dimensional heat flux ($F_{H\ \mathrm{dim}}$) as a function of dimensional time (t, in hours) for the one-layer 3-D DNS with $Pr = 13$, $\tau = 0.005$, and $R_\rho = 4$. After an initial period ($t < 2.2$ h) of strong flux growth, the system reaches a state of quasi-equilibrium, with fluxes fluctuating about the mean value $\overline{F_{H\ \mathrm{dim}}} = 0.4298$ Wm^{-2}. (b) A comparison of heat fluxes (as a function of R_ρ) diagnosed from 3-D DNS (*crosses*) with estimates based on extant laboratory-derived flux laws—*dotted line*: *Kelley* [1990], *dash-dotted line*: *Marmorino and Caldwell* [1976]. For increasing R_ρ ($> \sim 3$), both laws increasingly underestimate F_H, with an approximate factor of two difference for $R_\rho > 5$. *Solid line*: A best fit of the form (1), (8).

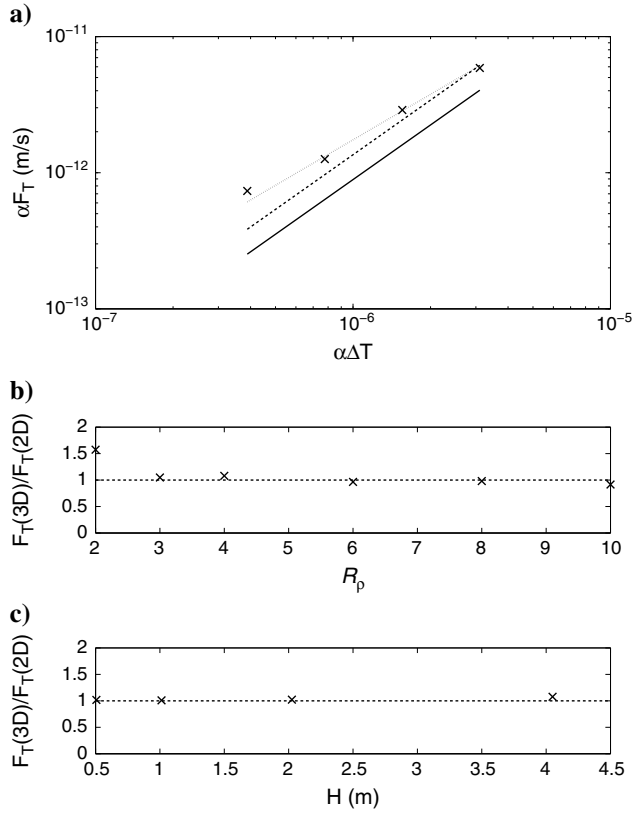

Figure 3. (a) Testing the "four-thirds flux law" exponent. *Crosses*: αF_T as a function of $\alpha\Delta T$ in logarithmic coordinates as diagnosed from 3-D DNS. *Solid line*: Heat Flux estimates from *Kelley's* [1990] law. *Dashed line*: A curve of the form (8), (1). *Dotted Line*: A curve of the form (8), (1) but with the exponent 1.11 in (1) instead of 4/3. (b and c) Comparisons of 2-D and 3-D DNS. Shown is the ratio $\overline{F_{T3D}}/\overline{F_{T2D}}$ for DNS with (Figure 3b) varying R_ρ and fixed H and (Figure 3c) varying H and fixed $R_\rho = 4$.

10% of the DNS value, with *Marmorino and Caldwell's* [1976] law performing at a similar level for $R_\rho = 3$. However, for larger R_ρ ($> \sim 3$), both laws underestimate F_H, with the discrepancy increasing with R_ρ—an approximate factor of two difference can be seen at large values of density ratio ($R_\rho > 5$). This discrepancy is not surprising, given the substantial differences in the numerical and laboratory setup.

[14] In order to present our findings in explicit form, also presented in Figure 2b is the best-fit curve of the form (1) with

$$C(R_\rho) = a + b(R_\rho - 1)^c \tag{8}$$

where $a = 0.0157$, $b = 0.0505$, and $c = -1.24$.

[15] Note that the flux law (8) offers an adequate description of the numerical data provided that the dependence on temperature variation is well-described by the 4/3 power law (1). Whether or not this assumption is accurate can be questioned [e.g., *Kelley*, 1990; *Kelley et al.*, 2003]. In order to determine whether our numerical simulations are adequately represented by the 4/3 power law in (1), we performed a set of 4 one-step 3-D DNS with different dimensional step-heights: $H = 0.5, 1, 2$ and 4 m. We have assumed the same parameter values for each DNS ($Pr = 13$, $\tau = 0.005$, and $R_\rho = 4$) and maintained identical grid spacing. The increase in H for the fixed temperature gradient ($\bar{T}_z = 1.361 \times 10^{-2}\,^\circ\mathrm{Cm}^{-1}$) corresponds to the variation in ΔT, thus allowing systematic analysis of the corresponding pattern of variation of heat transport. In Figure 3a, we present a plot of $\alpha\overline{F_T}$ as a function of $\alpha\Delta T$ (dimensional units) in logarithmic coordinates as derived from our DNS (crosses) and as estimated by both our parameterization (8) (dashed line) and *Kelley's* [1990] law (solid line). From inspection of Figure 3a, it is immediately apparent that the 4/3 exponent does not accurately describe our results. A best-fit curve of the form $\log|\alpha\overline{F_T}| = c + m\log|\alpha\Delta T|$ yields $m = 1.02$, significantly less than the commonly assumed 4/3. Since typical step-height in Arctic staircases is 1-4m, the fit was also made so as to exclude the lowest $\alpha\Delta T$ (i.e. $H = 0.5$m) giving $m = 1.11$ with $a = 0.00092$, $b = 0.00298$ in (8). This second parameterization is also shown in Figure 3a (dotted line) and clearly illustrates that differences between lab-predicted fluxes and our parameterization are primarily attributable to the pre-factor $C(R_\rho)$ in (1). It also should be noted that laboratory flux estimates come close to the numerical values for relatively large ΔT (equivalent to large step heights H) but the two differ for relatively thin steps.

[16] 2-D DNS enjoy obvious advantage over 3-D DNS since they are less computationally expensive for realistic parameters. However, it is reasonable to question whether 2-D DNS provide adequate approximation to their 3-D counterparts. To test their accuracy, we have conducted 2-D DNS with identical parameter sets and resolutions to those 3-D DNS described above and recorded $\overline{F_T}$ for each. In Figures 3b and 3c, we present the ratio $\overline{F_{T3D}}/\overline{F_{T2D}}$ for the DNS with fixed H and varying R_ρ and for those with fixed $R_\rho = 4$ and varying H, respectively. Surprisingly, in both cases, 2-D DNS stand up quite well. For varying R_ρ (Figure 3b), the maximum value $\overline{F_{T3D}}/\overline{F_{T\,2D}} = 1.574$ occurs at $R_\rho = 2$. However, for larger R_ρ, 2-D estimates are within 10% of 3-D. A similar consistency of 2-D experiments with their 3-D counterparts is seen when the density ratio is kept constant ($R_\rho = 4$), and layer thickness H is systematically varied (Figure 3c).

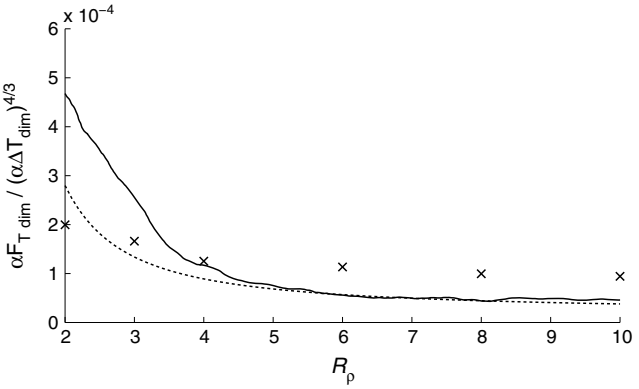

Figure 4. The effect of boundary conditions. Shown are heat fluxes as a function of R_ρ from 2-D DNS with rigid boundaries conditions (solid line) and from the equivalent 2-D DNS with periodic boundary conditions (crosses). As R_ρ increases, fluxes without boundaries are significantly higher than their rigid boundary counterparts. Also shown are flux estimates from *Kelley's* [1990] law (dashed line) that provides closer approximation to the rigid boundary flux values.

[17] To test the effects of boundaries, we have conducted a 2-D numerical experiment with rigid stress-free boundaries in both spatial directions (x,z), a setup that reflects the dynamics of laboratory run-down experiments. In this analysis, we have used the more efficient 2-D simulations since they were found to be generally adequate in capturing the dynamics of diffusive convection and the associated heat transport. To make the comparison between the periodic and run-down simulations objective, in both cases, we have utilized the same parameters ($Pr = 13,\ \tau = 0.005$), domain size (4m × 4m, dimensional), and resolution $(N_x,N_z) = (768,3072)$.

[18] The initial density ratio was $R_\rho = 1.5$, and, as the system ran down, R_ρ increased, which made it possible to calculate $\overline{F_T}$ as a function of R_ρ over the continuous range $1.5 < R_\rho < 10$. In Figure 4, we compare heat fluxes as a function of R_ρ from this DNS with those derived from the periodic 2-D simulations. To facilitate direct comparison with the extant flux laws, these fluxes were expressed in terms of the 4/3 flux law coefficient. In the run-down experiments, heat flux has been computed at the level of the diffusive interface ($z = H/2$) and smoothed in time using the running average interval of 20. For small values of R_ρ (< 3), fluxes with rigid boundaries are larger than those with periodic boundary conditions, with the difference rapidly diminishing as $R_\rho \to 3^-$. However, as R_ρ increases, the run-down fluxes fall significantly below the corresponding estimates from the periodic simulations. Additionally, we have included flux values as determined by *Kelley's* [1990] law. As is to be expected from a flux-law obtained in the laboratory setting (where rigid boundaries are present), *Kelley's* law provides better overall approximation to our run-down DNS-based flux values than the periodic system.

4. Conclusions

[19] In this manuscript, we have analyzed a set of DNS representing diffusive convection with periodic and rigid boundary conditions. The experiments were performed at unprecedented resolution, which made it possible for the first time to model the system with realistic parameters, matching the typical scales of the Beaufort Gyre staircase. Based on our diagnostics, we conclude the following:

[20] 1. The extant laboratory-derived flux laws are qualitatively consistent with numerical inferences but may underestimate the vertical heat transport by as much as a factor of two. An alternative DNS-based flux law is formulated.

[21] 2. The exponent of *Turner's* [1965] four-thirds flux law does not offer an optimal description of the numerical data. Evidence that the 4/3 exponent in (1) may require downward adjustment is provided.

[22] 3. Realistic 3-D simulations, which are inherently computationally expensive, are consistent with the equivalent 2-D DNS. The latter can provide an attractive alternative for sufficiently large R_ρ but the margin of error increases with decreasing R_ρ.

[23] 4. The choice of boundary conditions (rigid versus periodic) and the experimental setup (run-down versus maintained) has a substantial effect on the vertical heat transport.

[24] The rigid boundaries and/or run-down character of experiments act to significantly suppress the vertical heat transport. Since rigid bottom and side-walls are present in laboratory experiments, the application of the laboratory-derived flux laws to oceanic interfaces, which are not constrained by rigid boundaries and which can persist for years, may not be appropriate. It is suggested that oceanic staircases are better represented by models with maintained periodic boundary conditions. Based on our high-resolution experiments with periodic boundary conditions, we estimate that the error of extant flux laws is modest (a factor of two or less) and could be tolerated in many applications. However, if a more accurate estimate of the vertical heat transport is needed, we suggest using the flux law (8) based on the periodic simulations.

[25] **Acknowledgments.** This research was performed while J.F. held a National Research Council Award at the Naval Postgraduate School, Monterey. T. R. is supported by the NSF (CBET0933057 and ANT0944536). This work used the Extreme Science and Engineering Discovery Environment (XSEDE), which is supported by National Science Foundation grant number OCI-1053575. The authors thank Dan Kelley and an anonymous reviewer for their comments.

[26] The Editor thanks Dan Kelley and an anonymous reviewer for their assistance in evaluating this paper.

References

Caro, G. P. (2009), Direct numerical simulations of diffusive staircases in the Arctic. M.S. thesis, Dept. of Oceanography, Naval Postgraduate School, pp 61.

Carpenter, J. R., T. Sommer, and A. Wüest (2012), Simulations of a double-diffusive interface in the diffusive convection regime, *J. Fluid Mech.*, *771*, 411–436.

Kelley, D. E. (1990), Fluxes through diffusive staircases: A new formulation, *J. Geophys. Res.*, *95*, 3365–3371.

Kelley, D. E., H. J. S. Fernando, A. E. Gargett, J. Tanny, and E. Ozsoy (2003), The diffusive regime of double-diffusive convection, *Prog. Oceanogr.*, *56*, 461–481.

Krishfield R, K. Doherty, D. Frye, T. Hammar, J. Kemp, D. Peters, A. Proshutinsky, J. Toole, and K. von der Heydt (2006), Design and operation of automated Ice-Tethered Profilers for real-time seawater observations in the polar oceans. *Woods Hole Oceanographic Institution Tech. Rep*. WHOI-2006-NN, 30 pp.

Kwok, R., and N. Untersteiner (2011), The thinning of Arctic sea ice, *Physics Today*, *64*, 36-41.

Linden, P. F., and T. G. L. Shirtcliffe (1978), The diffusive interface in double-diffusive convection, *J. Fluid Mech.*, *87*, 417–432.

Marmorino, G. O., and D. R. Caldwell (1976), Heat and salt transport through a diffusive thermohaline interface, *Deep Sea Res.*, *23*, 59–67.

Stern, M. E., and T. Radko (1998), The salt finger amplitude in unbounded T-S gradient layers, *J. Mar. Res.*, *56*, 157–196.

Stern, M. E., T. Radko, and J. Simeonov (2001), 3D salt fingers in an unbounded thermocline with application to the Central Ocean, *J. Mar. Res.*, *59*, 355–390.

Timmermans, M. L., J. Toole, R. Krishfield, and P. Winsor (2008), Ice-Tethered Profiler observations of the double-diffusive staircase in the Canada Basin thermocline, *J. Geophys. Res.*, *113*, C00A02, doi:10.1029/2008JC004829.

Turner, J. S. (1965), The coupled turbulent transports of salt and heat across a sharp density interface, *Int. J Heat Mass Tran.*, *8*, 759–767.

Turner, J. S. (1973), *Buoyancy Effects in Fluids*, Cambridge University Press, Cambridge, pp. 367.

Turner, J. S. (2010), The melting of ice in the Arctic Ocean: The influence of double-diffusive transport of heat from below, *J. Phys Oceanogr.*, *40*, 249–256.